Electron localization of H_2^+ in a dc electric field*

Z M Jia(贾正茂)[1], Z N Zeng(曾志男)[1,†], W T Tang(唐文涛)[2], and R X Li(李儒新)[1]

[1] State Key Laboratory of High Field Laser Physics, Shanghai Institute of Optics and Fine Mechanics, Chinese Academy of Sciences, Shanghai 201800, China
[2] Signal and Information Processing, Jingchu University of Technology, Jingmen 448000, China

(Received 20 July 2016; revised manuscript received 27 September 2016; published online 30 November 2016)

A dc electric field is utilized to steer the electron motion after the molecular ion H_2^+ is excited by an ultrashort ultraviolet laser pulse. The numerical simulation shows that the electron localization distribution and the dissociation control ratio are dependent on the polarization direction and amplitude of the dc electric field. Most electrons of the dissociation state move opposite to the dc electric field and stabilize at the dressed-up potential well, for the dressed-down well is occupied by the electrons of the $1s\sigma_g$ state.

Keywords: dissociation localization, time dependent Schrödinger equation, Coulomb potential, ultraviolet laser pulse

PACS: 32.80.Rm, 33.80.Rv, 42.50.Hz, 42.65.Ky **DOI:** 10.1088/1674-1056/26/1/013201

1. Introduction

Coherent control of electrons and fragments in chemical reactions and photoelectron processes has attracted a great deal of interest. One of the main goals has been to find a way to selectively break and form molecular bonds in photochemical reactions.[1–3] As for searching for the underlying mechanism in realizing electron localization control during the dissociation process, several solution routes have been proposed, which include the mixture of the $1s\sigma_g$ and $2p\sigma_u$ states,[4] the interference between the $2p\sigma_u$ and $3s\sigma_g$ states,[5] the superposition of the $2p\pi_g$ and $2p\pi_u$ states,[6] and so on. In addition, the other quantum coupled equations[7–9] or laser-induced Stark shift effect[10–12] have also been used to reveal the dissociation control mechanism.

The hydrogen molecular ion is of special interest since it is the simplest molecule, consisting of three particles only. Even so, it plays an important role in the theoretical and experimental studies of electron localization in the dissociation of molecules. When the distance of the two protons of H_2^+ is small enough, the electron on the dissociation state can oscillate between them. With the increase of the distance, the inter-nuclear potential barrier would suppress such an oscillating behavior until the electron localization is stabilized.[13] In this paper, we utilize a dc electric field to steer the electron motion between the two protons after an ultrashort ultraviolet (UV) laser pulse is used to excite the electron wave packet onto the dissociation $2p\sigma_u$ state. Both the UV and dc electric fields are linearly polarized. The polarization direction of the UV pulse is along the molecular axis. The results show that the electron localization distribution and the electron dissociation control ratio are obviously dependent on the polarization direction and amplitude of the dc electric field. By adjusting the cross angle between the polarization axis of the dc electric field and the molecular axis, a probability as high as 98.8% to localize electrons on one of the two protons can be obtained, with a total dissociation probability of 53.9% and an ionization probability of 3.37%. Furthermore, for the electrons of the dissociation state, they move opposite to the dissociation control electric field (the dc electric field) and stabilize at the potential well which is dressed-up due to the occupation of the dressed-down potential well with the electrons of the $1s\sigma_g$ state.

This paper is organized as follows. Section 2 describes briefly the model system of H_2^+ and the parameters of the external electric fields we are using. In Section 3, the numerical results for the exploration of the control landscape of electron dynamics is studied. The physical mechanism underlying the localization is demonstrated in Section 4 with a simplified model. Finally, Section 5 contains a brief summary and the conclusion.

2. Simulation model

The polarization direction of the electric field component of the UV laser pulse is assumed to be parallel to the molecular axis, while the cross angle between the polarization axis of the dc electric field and the molecular axis varies from 0.0 to 2.0π, therefore, we can adopt the two-dimensional non-Born–Oppenheimer time-dependent Schrödinger equation (TDSE) to do the simulation. The corresponding TDSE can be written as ($e = \hbar = 1.0$ in atomic unit (a.u.), which are used throughout the paper unless otherwise stated)[6]

$$\mathrm{i}\frac{\partial}{\partial t}\varphi(R,z,x;t) = [T(R,z,x) + V_0(R,z,x) + W(z,x,t)]\varphi(R,z,x;t), \quad (1)$$

*Project supported by the National Natural Science Foundation of China (Grant Nos. 11127901, 61521093, 11134010, 11227902, 11222439, and 11274325) and the National Basic Research Program of China (Grant No. 2011CB808103).

†Corresponding author. E-mail: zhinan_zeng@mail.siom.ac.cn

© 2017 Chinese Physical Society and IOP Publishing Ltd

where $T(R,z,x)$ is the field-free Hamiltonian of the system, $V_0(R,z,x)$ stands for the soft-core Coulomb interaction, $W(z,x,t)$ indicates the interaction of the particle with the external laser pulse, R is the relative internuclear distance, and z and x collectively represent the electronic coordinates with respect to the center of mass of the two nuclei, as shown in Fig. 1.

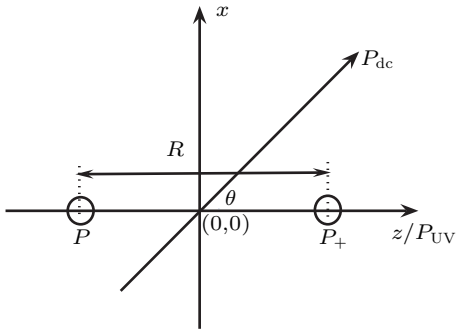


Fig. 1. The 2-dimensional model for H_2^+ molecular ion in the calculation, where R is the relative internuclear distance, and θ is the cross angle between the polarization axis of the dc electric field P_{dc} and the molecular axis. The electronic axes z and x are parallel and perpendicular to the molecular axis, respectively.

For our model, the kinetic energy in Eq. (1) reads

$$T(R,z,x) = -\frac{1}{m_p}\frac{\partial^2}{\partial R^2} - \left(\frac{2m_p+m_e}{4m_p m_e}\right)\frac{\partial^2}{\partial z^2} - \left(\frac{2m_p+m_e}{4m_p m_e}\right)\frac{\partial^2}{\partial x^2}, \quad (2)$$

the electronic axes z and x are assumed to be parallel and perpendicular to the molecular axis, respectively. Then the Coulomb potential of the system can be expressed as

$$V_0(R,z,x) = -\frac{1}{\sqrt{(z+R/2)^2+x^2}} - \frac{1}{\sqrt{(z-R/2)^2+x^2}} + \frac{1}{R}. \quad (3)$$

Here m_e and m_p are the electron and proton masses ($m_e = 1.0$, $m_p = 1837.0$), respectively.

The interaction of the system with the external laser field can be presented as

$$W(z,x,t) = \left(1+\frac{m_e}{2m_p+m_e}\right) \times [z(E_{UV}(t) + E_{dc}\cos(\theta)) + xE_{dc}\sin(\theta)]. \quad (4)$$

Here $E_{UV}(t)$ and E_{dc} stand for the electric component of the UV laser field and the dc electric field adopted in the simulation, respectively. θ is the cross angle between the axis of the molecular and the polarization of the dc electric field; more details can be found in Fig. 1.

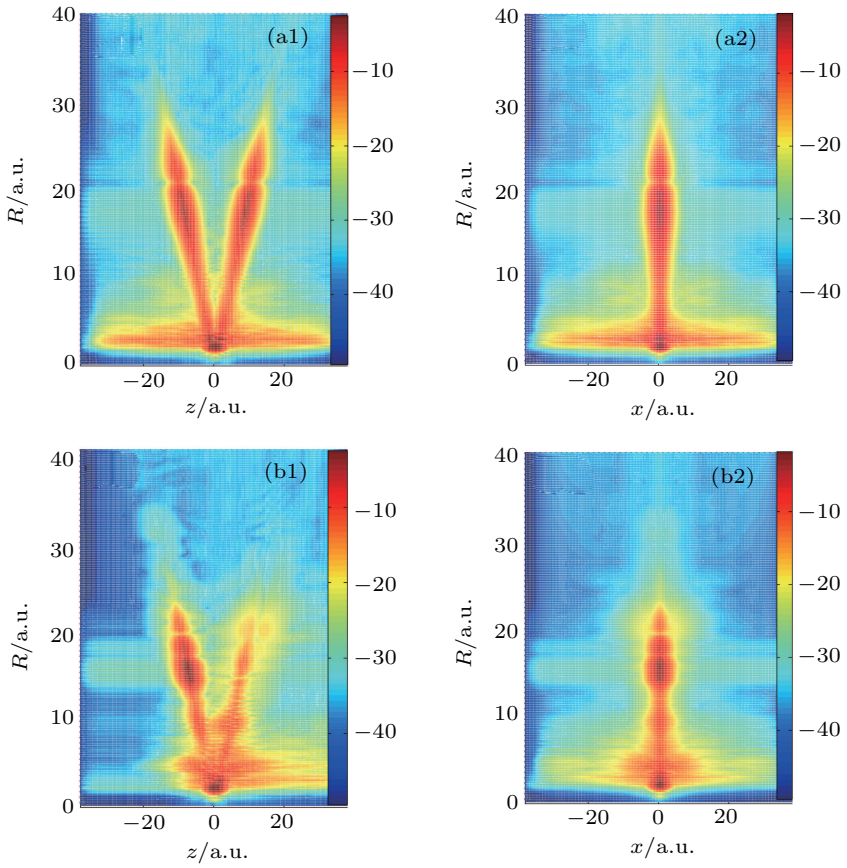


Fig. 2. (color online) Snapshots of the common logarithm of the electron-nuclear probability density distribution in the presentations of (z,R) and (x,R) spaces, taken at the end of the simulation: (a) only the UV pulse with an intensity of 2.0×10^{14} W/cm^2 is applied, (b) both the UV pulse and the dc electric field with an amplitude of -0.008 a.u. are utilized. The cross angle between the polarization axis of the dc electric field and the molecular axis is $\theta = 0.0$.

The time dependent electric field component of the UV pulse is given as $E_{\rm UV} = E_0 \sin(\pi t/T)^2 \sin(\omega t)$. Here E_0 is the peak electric field amplitude in atomic units, T is the pulse duration, and ω is the central frequency of the UV laser pulse. The four channels of H_2^+ dissociation are defined as[14–16]

$$P_z^+ = \int_{5.0}^{R_{\max}} {\rm d}R \int_{-x_{\max}/2.0}^{x_{\max}/2.0} {\rm d}x \int_{0.0}^{z_{\max}/2.0} {\rm d}z |\varphi(R,z,x;t_{\rm end})|^2,$$
$$P_z^- = \int_{5.0}^{R_{\max}} {\rm d}R \int_{-x_{\max}/2.0}^{x_{\max}/2.0} {\rm d}x \int_{-z_{\max}/2.0}^{0.0} {\rm d}z |\varphi(R,z,x;t_{\rm end})|^2,$$
$$P_x^+ = \int_{5.0}^{R_{\max}} {\rm d}R \int_{-z_{\max}/2.0}^{z_{\max}/2.0} {\rm d}z \int_{0.0}^{x_{\max}/2.0} {\rm d}x |\varphi(R,z,x;t_{\rm end})|^2,$$
$$P_x^- = \int_{5.0}^{R_{\max}} {\rm d}R \int_{-z_{\max}/2.0}^{z_{\max}/2.0} {\rm d}z \int_{-x_{\max}/2.0}^{0.0} {\rm d}x |\phi(R,x,z;t_{\rm end})|^2, \quad (5)$$

where $R_{\max}$, $z_{\max}$, and $x_{\max}$ correspond to the boundaries of the R, z, and x axes, and $\varphi(R,z,x;t_{\rm end})$ is the final wave function of the system. In the simulation, $t_{\rm end}$ is taken at 34.4 fs after the on-set of the UV pulse, when the probabilities of the electron being localized on one of the protons (left – or right +, see Fig. 2) are stable.

In the simulation, the 140-nm UV pulse with an intensity of 2.0×10^{14} W/cm^2 and a pulse duration T of 15.9 fs is used to excite the electron wave packet onto the dissociative state $2p\sigma_u$. Then the dc electric field with an amplitude of -0.008 a.u. is used to steer the electron motion. This dc electric field does not induce any further ionization. In the calculation, we set the dissociation asymmetry parameter as $A = (P_z^+ - P_z^-)/(P_z^+ + P_z^-)$.

3. Simulation results and discussion

Figure 2 depicts the snapshots of the common logarithm of the electron–nuclear probability density distribution $D(z,R;t_{\rm end})$ and $D(x,R;t_{\rm end})$ in the (z,R) and (x,R) spaces, taken at the end of the dissociation ($t_{\rm end} = 34.4$fs) without or with the dc electric field, respectively,

$$D(R,z,t_{\rm end}) = \int_{-x_{\max}/2.0}^{x_{\max}/2.0} {\rm d}x |\varphi(R,z,x;t_{\rm end})|^2,$$
$$D(R,x;t_{\rm end}) = \int_{-z_{\max}/2.0}^{z_{\max}/2.0} {\rm d}z |\varphi(R,z,x;t_{\rm end})|^2. \quad (6)$$

One can find that the electron localization starts from about $R = 5.0$ a.u., therefore, the on-set of the R axis is 5.0 a.u. in the definition of dissociation channels of Eq. (5). From Fig. 2(a), one can see that a single UV pulse induces a symmetric electron distribution, both in the z and x directions, with $P_z^- = P_z^+ = 0.2482$ and $P_x^- = P_x^+ = 0.2482$, respectively, due to the symmetric distribution of the double-well coulomb potential of the molecular ion H_2^+. The total ionization probability is $I = 0.0231$, i.e., $I = 1.0 - E_{\rm sr}$, where

$$E_{\rm sr} = \int_{0.0}^{R_{\max}} {\rm d}R \int_{-z_{\max}/2.0}^{z_{\max}/2.0} {\rm d}z \int_{-x_{\max}/2.0}^{x_{\max}/2.0} {\rm d}x |\varphi(R,x,z;t_{\rm end})|^2$$

is the electron survival probability.

When a dc electric field, whose polarization is assumed to be parallel to the molecular axis, with an amplitude of -0.008 a.u. is utilized to steer the electron motion after the excitation of the UV pulse, the symmetric electron localization distribution along the z direction is seriously broken, which can be seen in Fig. 2(b1) (the cross angle between the polarization axis of the dc electric field and the molecular axis is $\theta = 0.0$). This is because along the z direction, the energies of the double-well Coulomb potential of the H_2^+ molecular ion are dressed up and down by the dc electric field due to the dipole interaction term $W(z,x,t)$. The energies of the right potential well are effectively descended by $|RE_{\rm dc}|/2$, while for the left well, the energies are ascended by $|RE_{\rm dc}|/2$. The direction of $\boldsymbol{E}_{\rm dc}$ is right, and the electric field force of the electron is in the right direction, as the charge on the electron is $e = 1.0$ in the simulation. While for the electrons on the dissociative state $2p\sigma_u$, they move opposite to the electric field force and stabilize at the dressed-up potential well (the left well). When the dissociation control electric field is in the right direction (a minus electric field), the electrons of the $1s\sigma_g$ state are mainly localized at the potential well with dressed-down energies, i.e., the right potential well. While for the electrons of the dissociation $2p\sigma_u$ state, most of them are stabilized at the left potential well which is dressed up, see Fig. 3. For the electrons of the $1s\sigma_g$ state, they are stabilized at the bound states of H_2^+ finally, because the $1s\sigma_g$ state is bounded. While for the electrons of the $2p\sigma_u$ state, most of them are localized at the left proton at the end of the simulation, for the $2p\sigma_u$ state is the first dissociative state of H_2^+. When the location probabilities are stable, one can obtain $P_z^- = 0.532$, $P_z^+ = 0.0067$, $I = 0.0337$, and $A = -0.975$. Thus 98.8% electrons of all the dissociation events along the z axis are localized at the left proton.

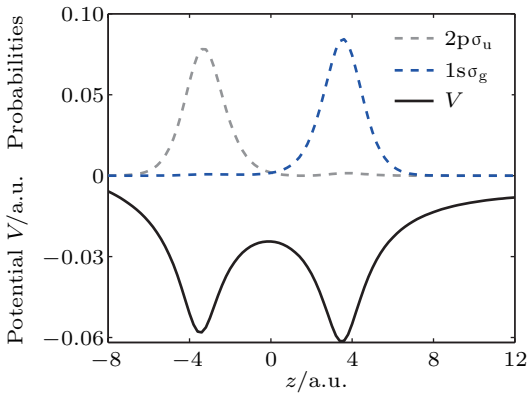


Fig. 3. (color online) The probabilities of the electron localization of the $1s\sigma_g$ and $2p\sigma_u$ states of H_2^+ on the double Coulomb potential wells along the z axis. Both the UV pulse with an intensity of 2.0×10^{14} W/cm^2 and the dc electric field with an amplitude of -0.008a.u. are applied. The cross angle between the polarization axis of the dc electric field and the molecular axis is $\theta = 0.0$.

For the electron localization distribution along the x direction, there lies a symmetric distribution with $P_x^- = P_x^+ =$

0.2693, as can be found in Fig. 2(b2), due to the symmetric distribution of the Coulomb potential wells along this direction.

Figure 4 shows the dissociation asymmetry parameter A, the total ionization probability I, and the probabilities of the electron being localized on the left (or right) proton P_z^- (or P_z^+) as functions of θ, the cross angle between the polarization axis of the dc electric field and the molecular axis. The amplitude of the dc electric field is $E_{\rm dc} = -0.008$ a.u. The intensity of the 140-nm UV laser pulse is 2.0×10^{14} W/cm^2. From this figure, one can find that the polarization direction of the dc electric field plays a very important role in the electron localization distribution. The largest dissociation control ratio can be obtained when the polarization is parallel to the molecular axis, i.e., when the cross angles are $\theta = 0.0$ and π, the dissociation asymmetry parameters are $A = -0.975$ and 0.972, respectively. 98.8% and 98.6% electrons of all the dissociation events can be steered onto the left or right proton, respectively, due to the dressing effect of the dc electric field. When the cross angle is $\theta = 0.0$, the left potential well is dressed-up. When $\theta = \pi$, the dressed-up potential well is the right one. For the electrons of the dissociation state $2p\sigma_u$, most would move opposite to the dc electric field and stabilize at the ascended potential well at the end of the simulation, as mentioned above.

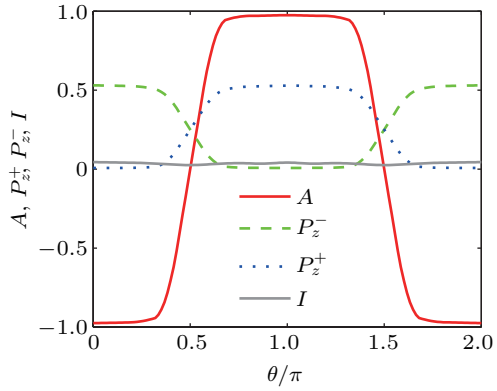


Fig. 4. (color online) The dissociation asymmetry parameter A, the total ionization probability I, and $P_z^{\pm}$ as functions of θ, the cross angle between the polarization axis of the dc electric field and the molecular axis. The amplitude of the dc electric field is -0.008 a.u. The intensity of the 140-nm UV pulse is 2.0×10^{14} W/cm^2.

The dissociation control ratio decreases with the polarization of the dc electric field changing from the parallel to the perpendicular direction of the molecular axis due to the weakening of the dressing effect of the dc electric field. When $\theta = \pi/2$ and $3\pi/2$, a symmetric electron localization distribution can be obtained with $P_z^- = P_z^+ = 0.2482$ and $P_z^- = P_z^+ = 0.2486$, respectively, as a result of the symmetric distribution of the Coulomb potential wells (the amplitude of the dc electric is 0.0).

Figure 5 shows the dissociation asymmetry parameter A, the total ionization probability I, and the probabilities of the electron being localized on the left (or right) proton P_z^- (or P_z^+) as functions of $E_{\rm dc}$, the amplitude of the dc electric field. The cross angle between the polarization axis of the dc electric field and the molecular axis is $\theta = 0.0$. The intensity of the 140-nm UV laser pulse is 2.0×10^{14} W/cm^2. When the amplitude of the dc electric field is between -0.004375 a.u. and -0.03275 a.u., $A \le -0.9$, more than 95% electrons of the dissociation $2p\sigma_u$ state can be steered onto the left proton and the total dissociation probability is larger than 34%. When $|E_{\rm dc}|$ is less than 0.004375 a.u., it is not strong enough to ensure a good electron-direction selection. If $|E_{\rm dc}|$ is higher than 0.03275 a.u., more electrons are excited onto the higher $3s\sigma$ state and the asymmetry parameter A decreases. Furthermore, more electrons are ionized with the increase of the absolute amplitude of the dc electric field. When $E_{\rm dc} = -0.004375$ a.u., the total ionization probability is $I = 0.02426$. When $E_{\rm dc} = -0.03275$ a.u., $I = 0.1113$. Therefore, the dc electric field with an absolute amplitude between 0.004375 a.u. and 0.03275 a.u. can be utilized to control the electron localization.

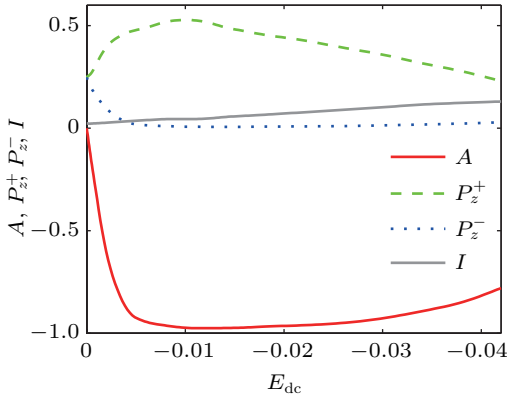


Fig. 5. (color online) The dissociation asymmetry parameter A, the total ionization probability I, and $P_z^{\pm}$ as functions of $E_{\rm dc}$, the amplitude of the dc electric field. The cross angle between the polarization axis of the dc electric field and the molecular axis is $\theta = 0.0$. The intensity of the 140-nm UV pulse is 2.0×10^{14} W/cm^2.

4. Simulation with analytical solution

In this section, the electron localization of the $1s\sigma_g$ and $2p\sigma_u$ states of a double-well Coulomb potential model system in an external dc electric field is demonstrated in detail with an analytical solution. The corresponding potential curve of the Coulomb potential can be expressed as[17]

$$V(z) = C^3Sz - C^2z^2/2 + z^4/4, \tag{7}$$

where C and S are constants, and the barrier height of the double-well potential is $C^4/4$.

The trial wave packet can be written as

$$\psi(z) = a\varphi_{\rm L}(z) + b\varphi_{\rm R}(z), \tag{8}$$

where $\varphi_{\rm L}(z) = \varphi(z+C)$ and $\varphi_{\rm R}(z) = \varphi(z-C)$ are the wave packets of the left and right potential wells, respectively, and

$\varphi(z) = \sqrt{2^{1/4}\sqrt{C}/\sqrt{\pi}}\,\mathrm{e}^{-\sqrt{2}Cz^2/2}$. The wave packets of the $1s\sigma_g$ (denoted as $|g\rangle$) and $2p\sigma_u$ ($|u\rangle$) states are

$$|g\rangle = a_1\varphi_R(z) + b_1\varphi_L(z),$$
$$|u\rangle = a_2\phi_R(z) + b_2\varphi_L(z). \quad (9)$$

By inserting Eqs. (7) and (8) into the Schrödinger equation $H(z)\psi(z) = E\psi(z)$ and making use of $H(z) = -\partial^2/\partial z^2/2 + V(z)$, the Schrödinger equation can be given as

$$\begin{vmatrix} H_{LL} - \Delta H_{LR} & H_{LR} - \Delta H_{RR} \\ H_{LR} - \Delta H_{LL} & H_{RR} - \Delta H_{LR} \end{vmatrix} \begin{vmatrix} a \\ b \end{vmatrix} = E(1-\Delta^2) \begin{vmatrix} a \\ b \end{vmatrix}, \quad (10)$$

with

$$\begin{aligned} \Delta &= \langle\varphi_L||\varphi_R\rangle = \exp(-\sqrt{2}C^3), \\ H_{LR} &= \langle\varphi_L|H|\varphi_R\rangle = \left|-C^4 + C/4/\sqrt{2} + 3/32/C^2\right|\Delta, \\ H_{LL} &= -C^4S - C^4/4 + C/\sqrt{2} + 3/32/C^2, \\ H_{RR} &= C^4S - C^4/4 + C\sqrt{2} + 2/32/C^2, \end{aligned} \quad (11)$$

where Δ and H_{LR} represent the overlap integral and the tunneling effect between the two potential wells, respectively, and H_{LL} and H_{RR} are the energy levels of these two potential wells. When

$$\begin{aligned} F &= C^4S, \\ f &= -C^4 + C/(4\sqrt{2}) + 3/(32C^2), \\ W &= -C^4/4 + C/\sqrt{2} + 3/(32C^2), \\ W &= -C^4/4 + C/\sqrt{2} + 3/(32C^2), \end{aligned} \quad (12)$$

one can obtain

$$\begin{aligned} H_{LR} &= f\Delta, \\ H_{RR} &= W + E, \\ H_{LL} &= W - E, \end{aligned} \quad (13)$$

where F is the external dc electric field, whose polarization direction is along the molecular axis. Then we can rewrite Eq. (10) with the representation as

$$\begin{vmatrix} W - F - \Delta^2 f - E(1-\Delta^2) & \Delta f - \Delta(W+F) \\ \Delta f - \Delta(W-F) & W + F - \Delta^2 f - E(1-\Delta^2) \end{vmatrix} \begin{vmatrix} a \\ b \end{vmatrix} = 0, \quad (14)$$

the electron localization of the left and right potential wells are

$$\begin{aligned} a_1^2 &= (F + \sqrt{F^2+B})^2/[A + (F + \sqrt{F^2+B})^2], \\ b_1^2 &= A/[A + (F + \sqrt{F^2+B})^2], \\ a_2^2 &= (F - \sqrt{F^2+B})^2/[A + (F - \sqrt{F^2+B})^2], \\ b_2^2 &= A/[A + (F - \sqrt{F^2+B})^2], \end{aligned} \quad (15)$$

where $A = (W - f - F)^2\Delta^2$ and $B = (W - f)^2\Delta^2$. $1 - \Delta^2 \approx 1$. a_1^2, a_2^2 and b_1^2, b_2^2 are the electron localization ratios of the $1s\sigma_g$ and $2p\sigma_u$ states on the left and right potential wells, respectively. The double-well potential is dependent on S. A large S will lead to a single potential well, so $S \le 4/27$ in the calculation. When $W - f \ge F$, $A = (W - f - F)^2\Delta^2 \approx (W - f)^2\Delta^2$, and $A \approx B$. The electron localization ratios of the $1s\sigma_g$ and $2p\sigma_u$ states on the right potential well can be expressed as

$$\begin{aligned} b_1^2 &= B/[B + (F + \sqrt{F^2+B})^2], \\ b_2^2 &= B/[B + (F - \sqrt{F^2+B})^2]. \end{aligned} \quad (16)$$

When the double-well potential is definite, B is a constant. The localization ratios are dependent on $(F + \sqrt{F^2+B})^2$ and $(F - \sqrt{F^2+B})^2$.

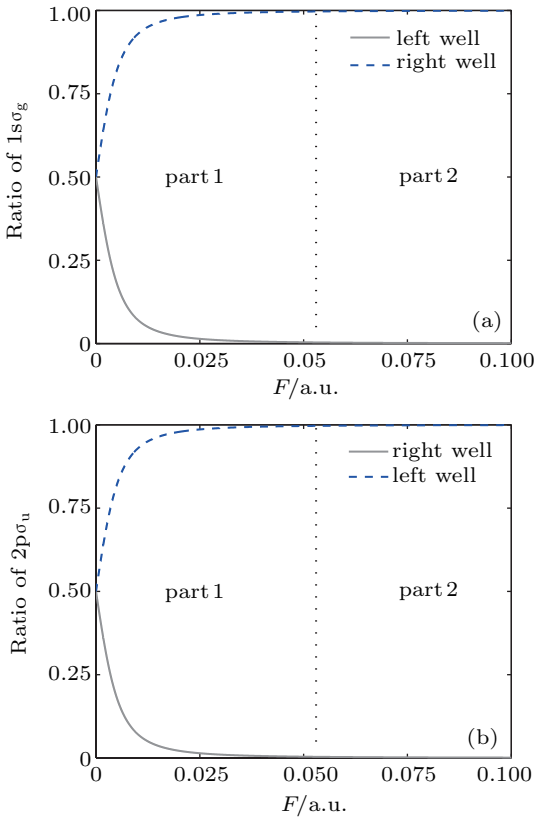


Fig. 6. (color online) Electron localization ratios of the $1s\sigma_g$ and $2p\sigma_u$ states on the left and right potential wells as functions of the amplitude of the external dc electric field.

When the amplitude of the external dc electric field is $F = 0.0$, $b_1^2 = b_2^2 = 0.5$, the electron distribution of the $1s\sigma_g$ and $2p\sigma_u$ states on the left and right potential wells is symmetric. With the increasing of F, b_1^2 decreases, the electron localization ratio of the $1s\sigma_g$ state on the right potential well decreases. For the electron localization ratio of the $2p\sigma_u$ state, with the increase of F, $\sqrt{F^2+B}$ increases too. While F increases faster than $\sqrt{F^2+B}$ and $F \le \sqrt{F^2+B}$, $b_2^2 = B/[B + (F - \sqrt{F^2+B})^2]$ increases with the increase of F. The electron localization ratio of the $2p\sigma_u$ state on the right potential well increases, as can be seen from part 1 in Fig. 6.

When $F^2 \gg B$, $\sqrt{F^2+B}$ is expanded in B/F^2, one can obtain

$$\sqrt{F^2+B} \approx F\left|1+B/(2F^2)\right|. \tag{17}$$

Then $b_1^2 \approx 0.0$ and $b_2^2 \approx 1.0$. For the $1s\sigma_g$ state, no electron localizes at the right potential well. For the $2p\sigma_u$ state, all the electrons are stabilized at the right potential well, as shown in part 2 in Fig. 6.

When the amplitude of the external dc electric field is $F < 0.0$, with the increase of $|F|$, b_2^2 decreases, the electron localization ratio of the $2p\sigma_u$ state on the right potential well decreases, and b_1^2 increases because $|F|$ increases faster than $\sqrt{F^2+B}$ and $|F| \leq \sqrt{F^2+B}$. The electron localization ratio of the $1s\sigma_g$ state on the right potential well increases. When $F^2 >> B$, one can obtain $\sqrt{F^2+B} \approx -F\left|1+B/(2F^2)\right|$. The electron localization ratios of the $1s\sigma_g$ and $2p\sigma_u$ states on the right potential well are $b_1^2 \approx 1.0$ and $b_2^2 \approx 0.0$. All the electrons of the $1s\sigma_g$ state and no electron of the $2p\sigma_u$ state are localized at the right potential well. With the same way, one can easily obtain that all the electrons of the $2p\sigma_u$ state are stabilized at the left potential well. The same conclusion can be obtained as the above TDSE.

5. Summary

We have shown the electron localization in the dissociation of H_2^+ molecular ion in a dc electric field after the excitation of a UV laser pulse. A high localization probability of 98.8% has been demonstrated when the polarization direction of the dc electric field is assumed to be parallel to the molecular axis. The total dissociation and ionization probabilities are 53.9% and 3.37%, respectively. For the electrons of the dissociation state $2p\sigma_u$, they move opposite to the dissociation control electric field force and stabilize at the dressed-up potential well due to the occupation of the dressed-down potential well with the electrons of the $1s\sigma_g$ state. The electron localization distribution and the dissociation control ratio are dependent on the polarization direction and amplitude of the dc electric field. The largest dissociation control ratio can be obtained when the polarization of the dc electric field is parallel to the molecular axis. When the polarization direction is perpendicular to the molecular axis, a symmetric electron distribution can be found due to the symmetric distribution of the Coulomb potential wells. A dc electric field, whose polarization is parallel to the molecular axis, with an absolute amplitude between 0.004375 a.u. and 0.03275 a.u. can be utilized to control the electron localization. When the amplitude of the dc electric field $|E_{dc}|$ is less than 0.004375 a.u., it is not strong enough to ensure a good electron-direction selection. If $|E_{dc}|$ is higher than 0.03275 a.u., more electrons of the ground state are excited onto the higher $3s\sigma$ state, and the dissociation control ratio decreases.

References

[1] Gaire B, McKenna J, Zohrabi M, Carnes K D, Esry B D and Ben-Itzhak I 2000 *Phys. Rev. A* **85** 023405

[2] Roudnev V and Esry B D 2007 *Phys. Rev. A* **76** 023403

[3] Vladimir R, Esry B D and Ben-Itzhak I 2004 *Phys. Rev. Lett.* **93** 163601

[4] McKenna J, Anis F, Sayler A M, Gaire B, Johnson Nora G, Parke E, Carnes K D, Esry B D and Ben-Itzhak I 2010 *Phys. Rev. A* **85** 023405

[5] Fischer B, Kremer M, Pfeifer T, Feuerstein B, Sharma V, Thumm U, Schröter C D, Moshammer R and Ullrich J 2010 *Phys. Rev. Lett.* **105** 223001

[6] He F 2012 *Phys. Rev. A* **86** 063415

[7] Kling M F, Siedschlag Ch, Znakovskaya I, Verhoef A J, Zherebtsov S, Krausz F, Lezius M and Vrakking M J J 2008 *Mole. Phys.* **106** 455

[8] Kling M F, Siedschlag Ch, Verhoef A J, Khan J I, Schultze M, Uphues Th, Ni Y, Uiberacker M, Drescher M, Krausz F and Vrakking M J J 2006 *Science* **312** 246

[9] Sansone G, Kelkensberg F, Pérez-Torres J F, Morales F, Kling M F, Siu W, Ghafur O, Johnsson, Swoboda P M, Benedetti E, Ferrari, Lépine F F, Sanz-Vicario J L, Zherebtsov S, Znakovskaya I, L'Huillier A, Ivanov M Yu, Nisoli M, Martín F and Vrakking M J J 2010 *Nature* **465** 763

[10] Dietrich P, Ivanov M Yu, Ilkov F A and Corkum P B 1996 *Phys. Rev. Lett.* **77** 4150

[11] Niikura Hiromichi, Corkum P B and Villeneuve D M 2003 *Phys. Rev. Lett.* **90** 203601

[12] Niikura Hiromichi, Villeneuve D M and Corkum P B 2004 *Phys. Rev. Lett.* **92** 133002

[13] He F, Ruiz C and Becker A 2007 *Phys. Rev. Lett.* **99** 083002

[14] Jia Z, Zeng Z, Li R, Xu Z and Deng Y 2014 *Phys. Rev. A* **89** 023419

[15] Jia Z, Zeng Z, Li R and Xu Z 2014 *Chin. Phys. B* **23** 083201

[16] Jia Z, Zeng Z, Li R, Xu Z and Deng Y 2015 *Chin. Phys. B* **24** 013204

[17] Cao D, Li Y, Bi D, Wang L and Cheng Y 2004 *Acta Phys. Sin.* **53** 2444 (in Chinese)